Boundary Conditions for Mode-Matching Analyses of Coupled Acoustic Fields in Ducts

Roy J. Beckemeyer* and David T. Sawdy†
Boeing Wichita Company, Wichita, Kansas

The mode-matching method is used to analyze sound propagation in ducts modeled by a series of segments. Successful application of the method depends on adequately specifying and imposing the boundary conditions used to match the acoustic fields on the junctions between segments. Although the boundary conditions may be derived by straightforward physical or mathematical arguments, the method by which they must be imposed in order to produce a well-posed numerical problem is not always clear. To illustrate this point, difficulties encountered when attempting to impose the matching conditions for a duct with a partial transverse baffle are discussed; several methods of approach are considered. Two of them were used to analyze a complicated duct-cavity system. Samples of the numerical results obtained are given.

Nomenclature

a = baffle height in folded cavity duct configuration
$a_n, a_{j,n}$ = complex coefficient giving amplitude and phase of the nth right-moving mode in the jth duct segment
b = height of cavity
$b_n, b_{j,n}$ = complex coefficients giving amplitude and phase of the nth left-moving mode in the jth duct segment
c = sound speed in medium
D_j = jth region or segment of duct
f = frequency, Hz
$f(j,n)$ = term in matching equations
F_{nm} = term in matching equations
g = baffle height
h, h_j = duct height, height of jth duct segment
i = $\sqrt{-1}$
k = wave number = $2\pi f/c$
ℓ = length of lined portion of folded cavity
L, L_j = length of duct segment, length of jth duct segment
M = number of left-moving modes in expansion
M_0 = Mach number of mean flow in duct
N = number of right-moving modes in expansion
p_j = acoustic perturbation pressure in jth duct segment
$r(j,n)$ = term in matching equations
$s(j,n)$ = term in matching equations
w_j = axial component of acoustic perturbation particle velocity
y = transverse coordinate
z, z_j = axial coordinate
$\alpha(n), \beta(n), \gamma(n), \delta(n)$ = terms in matching equations
ϵ = baffle thickness
ζ, ζ_L, ζ_U = face sheet impedance
λ_n = axial propagation constant for nth right-moving mode
$\vec{\lambda}_{j,n}$ = axial propagation constant for nth mode in jth duct segment; used with arrow to indicate modal propagation direction
μ_n = axial propagation constant for nth left-moving mode
$\vec{\vec{\mu}}^{l}_{j,n}$ = eigenvalue for jth segment, nth mode; superscript indicates whether region is above or below face sheet; used with arrow to indicate modal propagation direction
ρ = density of medium
ϕ_j = transverse eigenfunction, right-moving mode
ψ_j = transverse eigenfunction, left-moving mode
$\vec{\vec{\psi}}_n$ = weighting function for folded cavity eigenfunction expansion
ω = frequency, rad/s

Presented as Paper 78-194 at the AIAA 16th Aerospace Sciences Meeting, Huntsville, Ala., Jan. 16-18, 1978; submitted Feb. 8, 1978; revision received May 5, 1978.

Index categories: Noise; Aeroacoustics; Computational Methods.

*Research and Development Manager, Nacelle Branch. Member AIAA.

†Specialist Engineer, Noise Technology Staff.

Background and Introduction

SEVERAL quite sophisticated analyses and computer codes for studying sound propagation and attenuation in flow ducts of complicated configuration have been developed recently.[1-18] These procedures were developed in response to an increasing need for noise suppression in such high-technology devices as aircraft and lasers. The analyses commonly involve the use of numerical solution techniques and require the availability of large-scale computational facilities. Intended primarily for the investigation of sound propagation in ducts with segmented acoustic liners, these computer codes encompass a variety of analytical techniques, including mode-matching methods,[1-9] finite differences,[10,11] finite elements,[12-16] and, for certain duct configurations, numerical evaluation of explicit solutions.[17,18]

In this paper, we shall discuss certain aspects of the problem of successfully applying the mode matching method (also referred to as the eigenfunction expansion or modal superposition method), which is one of the most popular approaches currently in use for investigating segmented acoustic ducts. The widespread use of this technique undoubtedly is related to the fact that most of the early theoretical work on duct attenuation was based on investigations into the behavior of the lower-order mode or modes in

an infinite soft-walled duct. (A good example is the "least attenuated mode" theory of Cremer.[19]) As the theory of sound propagation in ducts advanced, Rice[20,21] used superposition of a number of lined ducts modes to investigate the behavior of plane waves in infinite soft-wall ducts. However, it was Zorumski[1,2] who was responsible in a large part for introducing the mode-matching method in its current form in which ducts with numerous liner segments are modeled by using a large number of forward- and backward-propagating modes to represent the field in each segment.

In the application of the mode-matching technique, ducts are divided into several regions or segments (Fig. 1), in each of which the Helmholtz equation and wall boundary conditions can be solved by separation of variables. Solution of the transverse component of the equations yields a set of eigenvalues and eigenfunctions that are superposed to represent the axial dependence of the acoustic field. The unknown coefficients that specify the relative amplitude and phase of each of the eigenfunctions in the modal expansions for the segment acoustic fields are determined by requiring field continuity from segment to segment, as well as satisfaction of any kinematic constraints on the boundaries between segments. Numerical difficulties encountered when applying mode matching to duct acoustics analyses usually are attributable to one of two causes: failure to insure that a complete set or a sufficient number of eigenfunctions are used in the modal expansion, or failure to adequately specify or impose the axial boundary conditions. In this paper, we deal with the latter problem. Although the authors of previous discussions were concerned with cases in which there were no structures normal to the duct walls,[2,4,7] in this study we shall consider boundary conditions complicated by the presence of transverse walls. In addition to presenting details of the boundary matching requirements and procedures, we have included examples of numerical results of studies of a specific baffled duct-cavity system. These results are validated by comparison with experimental data.

Boundary Condition Specification

For a given duct segment (see Fig. 1) in which the axial dependence of the acoustic field is represented by an expansion in terms of eigenfunctions, it is necessary to specify boundary conditions at each end of the segment to complete the solution for the acoustic field. Zorumski[1,2] and Unruh[7] have shown that impostion of conservation of acoustic perturbation mass and momentum at the ends of a duct segment of uniform height yields boundary conditions requiring continuity of pressure and axial acoustic particle velocity, respectively, across the end planes. A less physical, more mathematical viewpoint would be to recognize that imposition of pressure and axial velocity continuity corresponds to specification of Dirichlet and Neumann boundary data for the elliptic boundary-value problem within the duct segment. In either case, the boundary conditions are

$$p_j(z_j=0)=p_{j-1};\quad w_j(z_j=0)=w_{j-1} \tag{1}$$

$$p_j(z_j=L)=p_{j+1};\quad w_j(z_j=L)=w_{j+1} \tag{2}$$

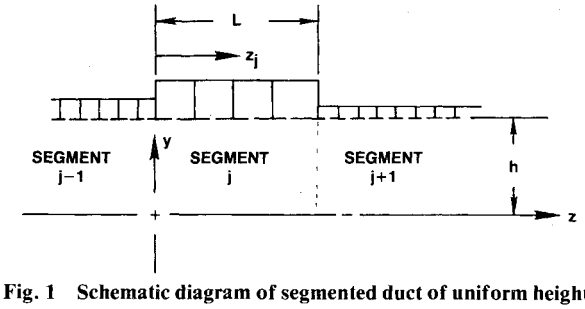

Fig. 1 Schematic diagram of segmented duct of uniform height.

It might appear at first glance that the boundary conditions, with both Neumann and Dirichlet data imposed on each boundary of the segment, are overspecified. The key, of course, is to recognize that we are dealing with a sequence of coupled boundary-value problems. One of each of the two sets of boundary conditions is associated with the boundary-value problem for duct segment j and the other two conditions with the problem for segments $j-1$ and $j+1$, respectively. For ducts of uniform height, it is arbitrary as to which condition is specified at each end of the segment. Suppose that for this case we choose to impose the equal pressure condition at the left boundary of segment j, and the equal axial particle velocity condition at the right boundary. Furthermore, let us suppose that the acoustic field in the segment is represented in terms of an eigenfunction expansion in terms of N right- and M left-propagating modes. Then the pressure and velocity may be written as

$$p_j=\sum_{n=0}^{N-1} a_n\phi_n(y)\exp(i\lambda_n z_j) + \sum_{n=0}^{M-1} b_n\psi_n(y)\exp[-i\mu_n(z_j-L)] \tag{3}$$

$$\rho c w_j=\sum_{n=0}^{N-1} a_n\lambda_n\phi_n(y)\exp(i\lambda_n z_j) - \sum_{n=0}^{M-1} b_n\mu_n\psi_n(y)\exp[-i\mu_n(z_j-L)] \tag{4}$$

Here the a_n are the complex coefficients for the right-moving modes and the b_n the coefficients for the left-moving modes. Applying the chosen boundary conditions, we obtain

$$p_j(z_j=0)=\sum_{n=0}^{N-1} a_n\phi_n(y)+\sum_{n=0}^{M-1} b_n\psi_n(y)\exp(i\mu_n L)=p_{j-1} \tag{5}$$

$$\rho c w_j(z_j=0)=\sum_{n=0}^{N-1} a_n\lambda_n\phi_n(y)\exp(i\lambda_n L) - \sum_{n=0}^{M-1} b_n\mu_n\psi_n(y)=\rho c w_{j+1} \tag{6}$$

To solve for the unknown coefficients a_n and b_n, we use the method of weighted residuals. Assuming that the eigenfunctions form a complete set of functions over the interval $-h\le y\le h$, we force the residual errors $\{p_j(z_j=0)-p_{j-1}\}$, $\{w_j(z_j=L)-w_{j+1}\}$ to be orthogonal to each eigenfunction ϕ_j and ψ_j for the pressure and velocity residuals, respectively, in turn, thus forcing the errors to vanish. This leads to a set of $(N+M)$ linear algebraic equations in the $(N+M)$ unknowns,

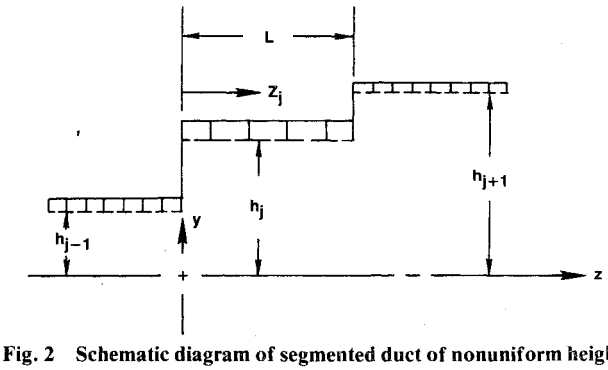

Fig. 2 Schematic diagram of segmented duct of nonuniform height.

a_n and b_n:

$$\sum_{n=0}^{N-1} a_n \int_{-h}^{h} \phi_n(y)\phi_m(y)\,dy + \sum_{n=0}^{M-1} b_n \exp(i\mu_n L) \int_{-h}^{h} \psi_n(y)\phi_m(y)\,dy = \int_{-h}^{h} p_{j-1}\phi_m(y)\,dy, \quad m=0,(1),N-1 \tag{7}$$

$$\sum_{n=0}^{N-1} a_n \lambda_n \exp(i\lambda_n L) \int_{-h}^{h} \phi_n(y)\psi_m(y)\,dy - \sum_{n=0}^{M-1} b_n \mu_n \int_{-h}^{h} \psi_n(y)\psi_m(y)\,dy = \rho c \int_{-h}^{h} w_{j+1}\psi_m(y)\,dy, \quad m=0,(1),M-1 \tag{8}$$

Note that, if the acoustic fields in the adjacent lining segments were also written in terms of modal expansions, the equation sets (7) and (8) would also contain as unknowns the coefficients for the expansions in segments $j-1$ and $j+1$. The equations needed to solve for the added unknown coefficients then would be provided by imposing velocity matching on the junction between segments $j-1$ and j and pressure matching on the boundary between segments j and $j+1$.[2-5]

For ducts with discontinuous cross-sectional changes (Fig. 2), the boundary matching becomes more complicated.[22,23] For these cases, although conservation of mass and momentum (or pressure and velocity) is again necessary for field continuity, there is an added kinematic condition: the velocity component normal to the transverse end walls must vanish. The appropriate boundary conditions are now[3,24,25]

$$p_j(y,0) = p_{j-1}(y,0), \quad 0 \le |y| \le h_{j-1} \tag{9a}$$

$$w_j(y,0) = \begin{cases} w_{j-1}(y,0), & 0 \le |y| \le h_{j-1} \\ 0, & h_{j-1} \le |y| \le h_{j+1} \end{cases} \tag{9b}$$

and

$$p_j(y,L) = p_{j+1}(y,L), \quad 0 \le |y| \le h_j \tag{10a}$$

$$w_{j+1}(y,L) = \begin{cases} w_j(y,L), & 0 \le |y| \le h_j \\ 0, & h_j \le |y| \le h_{j+1} \end{cases} \tag{10b}$$

In order to impose the kinematic condition of zero velocity on the end walls, it is now necessary that a specific boundary condition be associated with a specific duct segment or region.

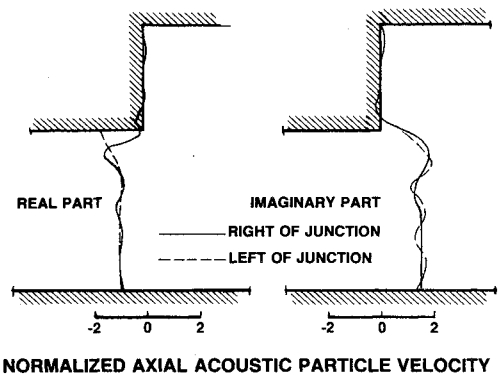

Fig. 3 Example of axial acoustic particle velocity distribution at a step in duct cross-sectional area.

Thus we *must* now append the velocity condition at the left end and the pressure condition at the right end to the boundary-value problem for segment j; *the choice of boundary data specification is no longer arbitrary*. The boundary conditions for segment j are thus

$$w_j(y,0) = \begin{cases} w_{j-1}(y,0), & 0 \le |y| \le h_{j-1} \\ 0, & h_{j-1} \le |y| \le h_j \end{cases} \tag{11a}$$

$$p_j(y,L) = p_{j+1}(y,L), \quad 0 \le |y| \le h_j \tag{11b}$$

which yield the algebraic equations

$$\sum_{n=0}^{N-1} a_n \lambda_n \int_{-h_j}^{h_j} \phi_n(y)\phi_m(y)\,dy - \sum_{n=0}^{M-1} b_n \mu_n \exp(i\mu_n L) \int_{-h_j}^{h_j} \psi_n(y)\phi_m(y)\,dy = -\int_{-h_{j-1}}^{h_{j-1}} w_{j-1}\phi_m(y)\,dy, \quad m=0,(1),N-1 \tag{12}$$

$$\sum_{n=0}^{N-1} a_n \exp(i\lambda_n L) \int_{-h_j}^{h_j} \phi_n(y)\psi_m(y)\,dy + \sum_{n=0}^{M-1} b_n \int_{-h_j}^{h_j} \psi_n(y)\psi_m(y)\,dy = \int_{-h_j}^{h_j} p_{j+1}\psi_m(y)\,dy, \quad m=0,(1),M-1 \tag{13}$$

It should be noted here that, as a result of this type of formulation of the boundary condition and matching equations, the zero normal velocity condition on the acoustically hard transverse walls is satisfied in an averaged sense (Fig. 3). That is, the value of the velocity oscillates about zero with a mean amplitude that nearly vanishes. Providing an adequate approximation of this discontinuous velocity distribution is a key factor in the successful modeling of the acoustics of flow ducts by mode matching.

The problem of imposing zero acoustical particle velocity on the transverse wall becomes more difficult when the wall takes the form of a baffle that only partially obstructs the duct (Fig. 4). In this case, the boundary conditions at the right-hand end of segment j are (Fig. 4)

$$w_j = w_{j+1}, \quad p_j = p_{j+1}, \quad g \le |y| \le h \tag{14a}$$

$$w_j = 0, \quad w_{j+1} = 0, \quad 0 \le |y| \le g \tag{14b}$$

The difficulty involves the need to simultaneously impose the zero velocity condition on the baffle in segment j and in segment $j+1$. Suppose that the Neumann condition is imposed in segment j so that we require w_j to be zero on the

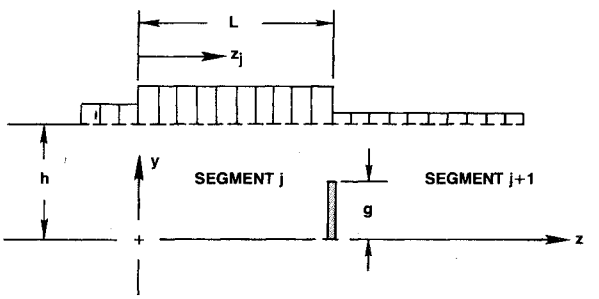

Fig. 4 Schematic diagram of segmented duct with partial transverse baffle between segments.

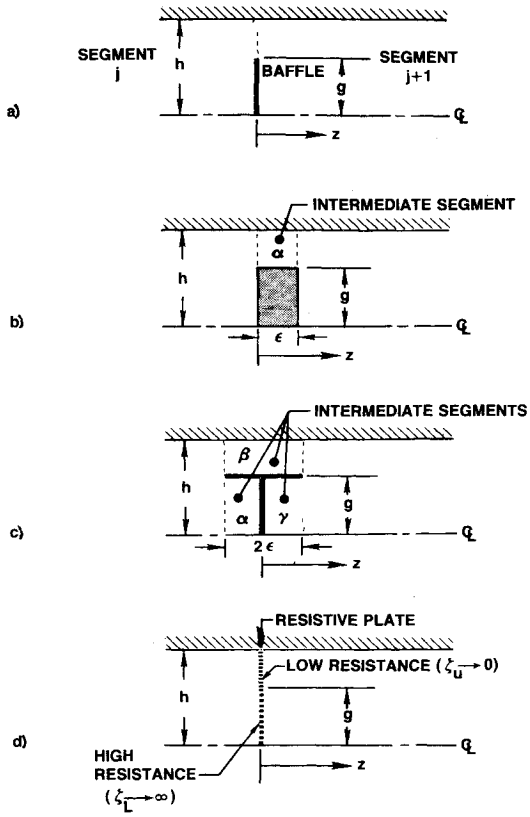

Fig. 5 Schematic of models used to approximate a partial baffle: a) actual geometry; b) and c) intermediate waveguide models; d) resistive plate model.

baffle and equal to w_{j+1} in the aperature. We are then left with a mixed boundary-value specification in segment $j+1$, with a Dirichlet condition ($p_j = p_{j+1}$) to be imposed in the aperature and a Neumann condition (w_{j+1}) on the baffle. There are conceptual difficulties associated with the imposition of these mixed boundary conditions in the mode-matching formulation: it is no longer clear with which segment boundary-value problem the full Neumann condition should be associated or with which segment the mixed condition should be associated. In addition, it is necessary to devise some type of hybrid cost function which includes the residual errors in pressure (on the aperature) and in velocity (on the baffle) in segment $j+1$. As a general rule, it has been our experience that these methods lead to numerical instabilities in the mode-matching solution process.[3,4] These numerical problems manifest themselves in the form of ill-conditioning of the coefficient matrix and failure of the coefficient values to converge as more modes are used in the expansions. In order to couple the acoustic fields of two segments separated by a partial baffle and simultaneously to impose the zero velocity condition on both sides of the baffle, we have found it necessary to develop alternate models for the baffle. These models allow the specification of a single boundary condition in each segment and avoid the numerical problems that occur when one attempts to impose mixed boundary conditions. Several of these models are shown in Fig. 5. Each of them allows the partial baffle to be approximated in a numerically satisfactory manner. The first two models (b and c in Fig. 5) involve the addition of intermediate waveguide segments. For these cases, the added segments remove the boundary condition ambiguity by once again making clear the appropriate choice of boundary data specification. Unfortunately, the simplification in specifying boundary conditions is offset to some degree by the addition of more unknowns: the coefficients used in the modal expansions of the fields in the intermediate segments. The boundary conditions for model b are

$$p_\alpha = p_j, \quad w_j = w_\alpha, \quad g \le |y| \le h, \quad z = 0 \tag{15a}$$

$$w_j = 0, \quad 0 \le |y| \le g, \quad z = 0 \tag{15b}$$

$$p_\alpha = p_{j+1}, \quad w_{j+1} = w_\alpha, \quad g \le |y| \le h, \quad z = \epsilon \tag{15c}$$

$$w_{j+1} = 0, \quad 0 \le |y| \le g, \quad z = \epsilon, \ \epsilon \to 0 \tag{15d}$$

By associating the pressure equivalence conditions with the boundary-value problem for the intermediate waveguide (segment α), sufficient equations are obtained so that the modal coefficients in the eigenfunction expansion for segment α can be expressed in terms of the coefficients for segments j and $j+1$. These equations then can be used to explicitly eliminate the modal coefficients for the intermediate segment from the total equation set.

The boundary conditions for model c (Fig. 5) can be written in a similar manner. Since this model is similar to model b but considerably more complicated, it was not investigated in detail. Model d (Fig. 5) results in a quite different set of boundary specifications at the baffle. In this case, we choose to model the baffle plane by a thin porous sheet, with high resistance in the region intended to model the impervious baffle and low resistance in the region of the aperature above the baffle. We then replace the Dirichlet (pressure equivalence) condition with a Cauchy or "third" boundary condition:

$$p_j - p_{j+1} = \begin{cases} \zeta_L w_j, & 0 \le |y| \le g, \quad z = 0 \\ \zeta_U w_j, & g \le |y| \le h, \quad z = 0 \end{cases} \tag{16}$$

and retain the inhomogeneous Neumann condition:

$$w_j = w_{j+1}, \quad 0 \le |y| \le h, \quad z = 0 \tag{17}$$

Note that, as $\zeta_U \to 0$ and $\zeta_L \to \infty$, Eqs. (16) and (17) approach Eqs. (14), since

$$w_j = w_{j+1} = [(p_j - p_{j+1})/\zeta_L] \to 0$$

$$\text{on} \quad 0 \le |y| \le g \quad \text{as} \quad \zeta_L \to \infty \tag{18a}$$

$$p_j - p_{j+1} = \zeta_U w_j \to 0 \quad \text{on} \quad g \le |y| \le h, \quad \text{as} \quad \zeta_U \to 0 \tag{18b}$$

Example of Boundary Matching

To illustrate the application of these approximations to a partial planar baffle in a duct,[24,25] models b and d were used to study the problem of sound propagation in a duct lined with a "folded cavity" liner (Fig. 6). To model the sound field in region D_2 (Fig. 6) of the duct, that segment was considered to be a hard-walled duct bifurcated by a porous sheet, with a uniform axial mean flow on one side of the bifurcation, but with zero axial flow on the other side.

The resulting expressions for the eigenvalue equation and the eigenfunction expansion for the field in D_2 are as follows:

Eigenvalue Equation

$$\mu_2^{II} \tan(\mu_2^{II} b) = \frac{-\mu_2^I \tan(\mu_2^I h)}{[(1 - \lambda_2 M_0/k)^2 + i\mu_2^I \zeta_F \tan(\mu_2^I h)]} \tag{19}$$

where

$$\mu_2^I = [(k - \lambda_2 M_0)^2 - (\lambda_2)^2]^{1/2}$$

$$\mu_2^{II} = [k^2 - (\lambda_2)^2]^{1/2}$$

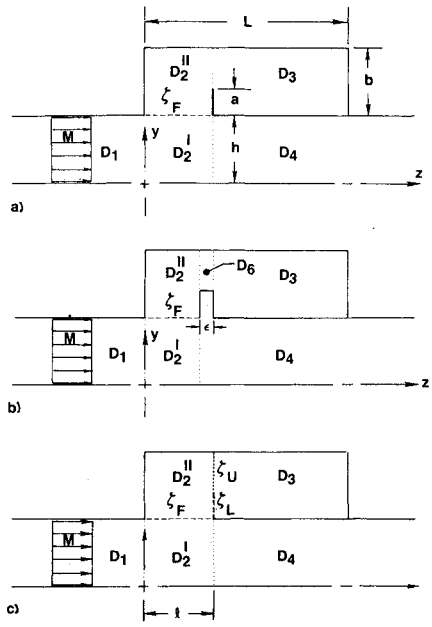

Fig. 6 Schematic diagrams of folded cavity duct lining: a) actual configuration; b) intermediate waveguide model; c) resistive sheet model.

Eigenfunction Expansion

$$p_2 = \begin{cases} p_2^I, & 0 \le |y| \le h \\ p_2^{II}, & h \le |y| \le h+b \end{cases} \tag{20a}$$

$$p_2^I = \sum_{n=0}^{N-1} a_{2,n} \cos(\vec{\mu}_{2,n}^I y) \exp(-i\vec{\lambda}_{2,n} z) + \sum_{n=0}^{M-1} b_{2,n} \cos(\check{\mu}_{2,n}^I y) \exp[-i\check{\lambda}_{2,n}(z-\ell)] \tag{20b}$$

$$p_2^{II} = \sum_{n=0}^{N-1} a_{2,n} \vec{\psi}_n \cos[\vec{\mu}_{2,n}^{II}(y-h-b)] \exp(-i\vec{\lambda}_{2,n} z) + \sum_{n=0}^{M-1} b_{2,n} \vec{\psi}_n \cos[\vec{\mu}_{2,n}^{II}(y-h-b)] \exp[-i\vec{\lambda}_{2,n}(z-\ell)] \tag{20c}$$

where

$$\psi_n = \frac{k\cos(\mu_{2,n}^{II} h)}{k\cos(\mu_{2,n}^{II} b) + i\zeta_F \mu_{2,n}^{II} \sin(\mu_{2,n}^{II} b)} \tag{21}$$

Note that p_2^I and p_2^{II} are discontinuous across the face sheet, and that the discontinuity in pressure is equal to the product of the face sheet impedance and the y component of acoustic particle velocity (which is continuous) through the face sheet.

Model b is applied to the folded cavity configuration by first imposing the conditions

$$p_6 = p_2^{II} \text{ on } h+a \le |y| \le h+b, \quad z=\ell \tag{22a}$$

$$p_6 = p_3 \text{ on } h+a \le |y| \le h+b, \quad z=\ell+\epsilon \tag{22b}$$

on the boundary-value problem for region D_6. These conditions yield expressions for the coefficients $a_{6,m}$ and $b_{6,m}$ for the field in region D_6 in terms of coefficients $a_{2,n}$, $b_{2,n}$, $a_{3,n}$, and $b_{3,n}$ for the fields in regions D_2 and D_3.

Finally, the boundary conditions for region D_3:

$$w_3 = 0, \quad h \le |y| \le h+b, \quad z=L \tag{23a}$$

$$w_3 = \begin{cases} 0, & h \le |y| \le h+a, \quad z=\ell+\epsilon \\ w_6, & h+a \le |y| \le h+b, \quad z=\ell+\epsilon \end{cases} \tag{23b}$$

are imposed, together with the right-hand boundary condition for region D_2:

$$w_2 = \begin{cases} w_2^I = w_4, & 0 \le |y| \le h, \quad z=\ell \\ w_2^{II} = \begin{cases} 0, & h \le |y| \le h+a, \quad z=\ell \\ w_6, & h+a \le |y| \le h+b, \quad z=\ell \end{cases} \end{cases} \tag{24}$$

We are particularly interested in the matching equation that arises from the "pressure equivalence" condition at $z=\ell$, which takes the form

$$\sum_n a_{2,n}\left[\sum_j \frac{f(j,n)}{\sin(\vec{\lambda}_{6,j}\epsilon)}\right] + \sum_n b_{2,n}\left[\sum_j \frac{g(j,n)}{\sin(\vec{\lambda}_{6,j}\epsilon)}\right] + \sum_n a_{3,n}\left[\frac{\vec{\lambda}_{3,n}F_{nm}}{k} - \sum_j\left(\frac{r(j,n)}{\sin(\vec{\lambda}_{6,j}\epsilon)}\right)\right] + \sum_n b_{3,n}\left[\frac{\check{\lambda}_{3,n}F_{nm}\exp\{-i\check{\lambda}_{3,n}(L-\ell-\epsilon)\}}{k} - \sum_j\left(\frac{s(j,n)}{\sin(\vec{\lambda}_{6,j}\epsilon)}\right)\right] = 0 \tag{25}$$

Note that, as ϵ is allowed to approach zero, so that the waveguide of region D_6 becomes a baffle, certain terms in the matching equation become dominant. A similar behavior is evident in the matching equation for model d. For this case, the boundary conditions for region D_3 are taken as

$$w_3 = 0, \quad h \le |y| \le h+b, \quad z=L \tag{26a}$$

$$w_3 = \begin{cases} (p_2^{II} - p_3)/\zeta_L, & h \le |y| \le h+a, \quad z=\ell \\ (p_2^{II} - p_3)/\zeta_U, & h+a \le |y| \le h+b, \quad z=\ell \end{cases} \tag{26b}$$

where $\zeta_L \to \infty$, $\zeta_U \to 0$, while the condition for the right-hand side of region D_2 is

$$w_2 = \begin{cases} w_2^I = w_4, & 0 \le |y| \le h, \quad z=\ell \\ w_2^{II} = w_3, & h \le |y| \le h+b, \quad z=\ell \end{cases} \tag{27}$$

The "pressure equivalence" condition for this case is of the form

$$\sum_n a_{2,n}\left\{\frac{\alpha(n)}{\zeta_U}\right\} + \sum_n b_{2,n}\left\{\frac{\beta(n)}{\zeta_U}\right\} + \sum_n a_{3,n}\left\{\frac{\vec{\lambda}_{3,n}F_{nm}}{k} + \frac{\gamma(n)}{\zeta_U}\right\} + \sum_n b_{3,n}\left\{\frac{\check{\lambda}_{3,n}F_{nm}\exp[-i\check{\lambda}_{3,n}(L-\ell)]}{k} + \frac{\delta(n)}{\zeta_U}\right\} = 0 \tag{28}$$

The similarity between this equation and Eq. (25) is quite striking. The limiting case $\zeta_U \to 0$ and $\epsilon \to 0$ cause similar terms in each equation to become dominant. In each case, the coefficients of the $a_{2,n}$ and $b_{2,n}$ increase in magnitude, whereas the F_{nm} terms in the coefficients of the $a_{3,n}$ and $b_{3,n}$ become less significant. This similarity in behavior indicated to us that results obtained using those models might be expected to be similar also. This has been borne out by our subsequent investigations. Obviously, model b has the advantage of appearing intuitively more satisfactory, since the model closely represents the actual baffled cavity. Model d,

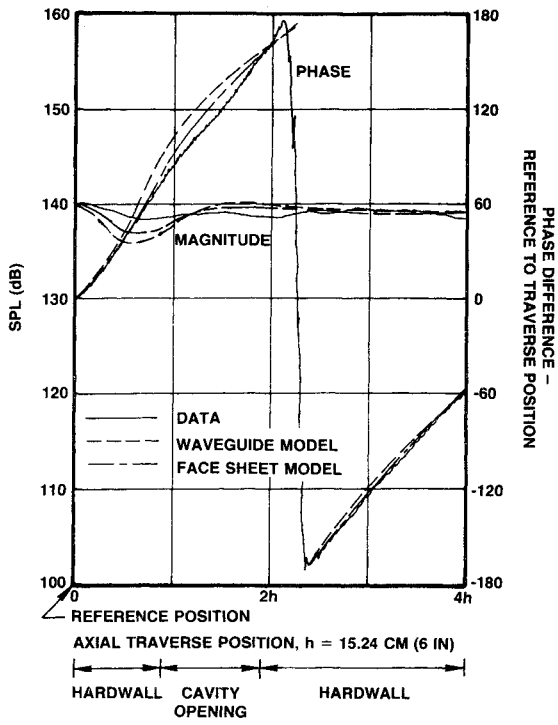

Fig. 7 Comparison of the measured axial distribution of acoustic pressure magnitude and phase for a folded cavity duct configuration with predictions made by use of models b and d.

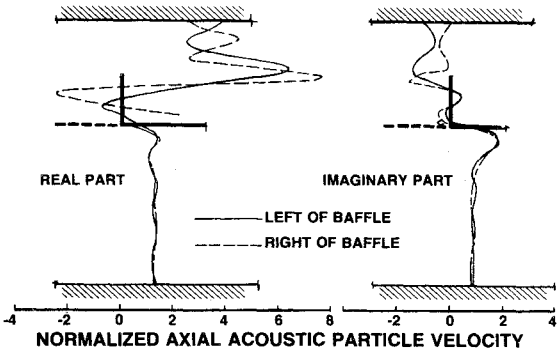

Fig. 8 Transverse distribution of axial acoustic particle velocity on plane of baffle as computed by use of model b.

on the other hand, is not so aesthetically pleasing; values taken for parameters ζ_U and ζ_L must be somewhat arbitrary, since the actual values are 0 and ∞. However, model d does offer the options of setting a value for ζ_U to account for any losses that actually might occur there, and of actually replacing the baffle by a face sheet. Consequently, both models have been incorporated in our folded cavity analyses.

Figures 7-9 contain typical results obtained using the two analyses. In Fig. 7, we show the excellent agreement between experimentally measured and analytically predicted sound pressure levels and phase variations for the acoustic pressure at the centerline of a symmetric duct containing a folded cavity. Pertinent dimensions and parameter values are $h=15.2$ cm (6.0 in.), $b=10.2$ cm (4.0 in.), $a=5.1$ cm (2.0 in.), $L=26.7$ cm (10.5 in.), $\ell=15.2$ cm (6.0 in.), $f=570$ Hz, $M_0=0.2$, $kh=1.578$. Parameter values for the models were $k\epsilon=0.0001$, $\zeta_U=0.005\rho c$, $\zeta_L=50.0\ \rho c$ ($k=2\pi f/c$, where c is the sound speed, ρc = characteristic impedance of air). Seven right-moving and seven left-moving modes were used to represent the acoustic fields in all duct segments except for segment α of model b (Fig. 6), for which 15 right- and 15 left-propagating modes were used. Figures 8 and 9 give computed axial acoustic particle velocity distribution on either side of

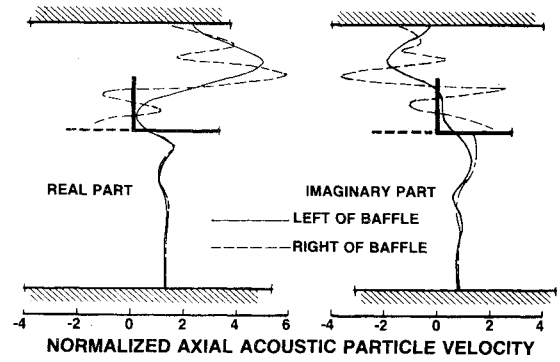

Fig. 9 Transverse distribution of axial acoustic particle velocity on plane of baffle as computed by use of model d.

the plane of the baffle as computed using models b and d, respectively. Pressure distributions are not shown because pressure data on interfaces invariably match to within graphical accuracy. Of particular interest in Figs. 8 and 9 is the manner in which the zero velocity is approximated on the baffle and the velocity matching is imposed between segments on the aperature above the baffle. In both cases, the velocities match in an average sense, oscillating about the mean or true value. As evidenced by the data in Fig. 7, both models provide an adequate approximation for the problem. (Additional comparisons of experimental and analytical data have been presented previously.[24,25])

Conclusions

The mode-matching method is a powerful technique for predicting the behavior of flow duct acoustic liners, but the accuracy that it provides is directly related to the adequacy of boundary condition specification and imposition. Boundary conditions may be derived by straightforward application of physical arguments related to conservation of mass and momentum or mathematical arguments related to the problem of adequately posing a boundary-value problem. However, it is sometimes necessary to improvise intricate methods with which to actually impose these boundary conditions.

References

[1] Lansing, D. L. and Zorumski, W. E., "Effects of Wall Admittance Changes on Duct Transmission and Radiation of Sound," *Journal of Sound and Vibration*, Vol. 27, Jan. 1973, pp. 85-100.

[2] Zorumski, W. E., "Acoustic Theory of Axisymmetric Multisectioned Ducts," NASA TR-R-419, 1974.

[3] Beckemeyer, R. J. and Eversman, W., "Computational Methods for Studying Acoustic Propagation in Nonuniform Waveguides," AIAA *Progress in Astronautics and Aeronautics—Aeroacoustics: Jet and Combustion Noise; Duct Acoustics*, Vol. 37, edited by H. T. Nagamatsu, N.Y., 1975, pp. 455-469.

[4] Sawdy, D. T., Beckemeyer, R. J., and Garner, P., "Effects of a Conical Segment on Sound Radiation from a Circular Duct," AIAA *Progress in Astronautics and Aeronautics—Aeroacoustics: Fan Noise & Control; Duct Acoustics; Rotor Noise*, Vol. 44, edited by I. R. Schwartz, N.Y., 1976, pp. 433-450.

[5] Sawdy, D. T., Beckemeyer, R. J., and Patterson, J. D., "Analytical and Experimental Studies of an Optimum Multisegment Phased Liner Noise Suppression Concept," NASA CR-134960, May 1976.

[6] Motsinger, R. E., Kraft, R. E., Zwick, J. W., Vubelich, S. I., Minner, G. L., and Baumeister, K. J., "Optimization of Suppression for Two-Element Treatment Liners for Turbomachinery Exhaust Ducts," NASA CR-134997, April 1976.

[7] Unruh, J. F., "Finite Length Tuning for Low Frequency Lining Design," *Journal of Sound and Vibration*, Vol. 45, Jan. 1976, pp. 5-14.

[8] Unruh, J. F. and Price, I. R., "Experimental Verification of a Finite Length Tuning Concept for Acoustic Lining Design," *Journal of Sound and Vibration*, Vol. 49, March 1976, pp. 393-402.

[9] Wyerman, B. R. and Reethof, G., "The Propation of Plane Waves and Higher Order Acoustic Modes in Multisectioned Ducts,"

Third Interagency Symposium on University Research in Transportation Noise, 1975.

[10] Quinn, D. W., "Attenuation of Sound Associated with a Plane Wave in a Multisectional Duct," AIAA *Progress in Astronautics and Aeronautics—Aeroacoustics: Fan Noise & Control; Duct Acoustics; Rotor Noise*, Vol. 44, edited by I. R. Schwartz, N.Y., 1976, pp. 331-345.

[11] Baumeister, K. D., "Wave Envelope Analysis of Sound Propagation in Ducts with Variable Axial Impedance," AIAA *Progress in Astronautics and Aeronautics—Aeroacoustics: Fan Noise & Control; Duct Acoustics; Rotor Noise*, Vol. 44, edited by I. R. Schwartz, N.Y., 1976, pp. 451-474.

[12] Craggs, A., "A Finite Element Method for Damped Acoustic Systems; An Application to Evaluate the Performance of Reactive Mufflers," *Journal of Sound and Vibration*, Vol. 48, 1976, pp. 377-391.

[13] Sigman, R. K., Majjigi, R. K., and Zinn, B. T., "Use of Finite Element Techniques in the Determination of the Acoustic Properties of Turbofan Inlets," AIAA Paper 77-18, Los Angeles, Calif., 1977.

[14] Watson, W. R., "A Finite Element Simulation of Sound Attenuation in a Finite Duct with a Peripherally Variable Liner," NASA TMX-74080, 1977.

[15] Eversman, W., Astley, R. J. and Thanh, V. P., "Transmission in Nonuniform Ducts—A Comparative Evaluation of Finite Element and Weighted Residual Computational Schemes," AIAA Paper 77-1299, Atlanta, Ga., 1977.

[16] Abrahamson, A. L., "A Finite Element Algorithm for Sound Propagation in Axisymmetric Ducts Containing Compressible Mean Flow," AIAA Paper 77-1301, Atlanta, Ga., 1977.

[17] Koch, W., "Schalldämpfung bei Mehrfachauskleidungen in Rechteckkanal unter Berücksichtigung der unstetigen Änderungen der Wandimpedanz," Deutsche Forschungs-und Versuchsanstalt fur Luft-und Raumfahrt, Göttingen, DLR-FB 76-07, 1976.

[18] Koch, W., "Exact Wiener-Hopf Solution of Multi-section Duct Liners," AIAA Paper 76-513, Palo Alto, Calif., 1976.

[19] Cremer, L., "Theorie der Luftschall-Dampfung in Rechtekanal mit Schuckender Wand und das sich dabei Ergebende hochste Dampfungsmass," *Acustica*, Vol. 3, 1953, pp. 249-263.

[20] Rice, E. J., "Attenuation of Sound in Soft-Wall Ducts," NASA TMX-52442, 1968.

[21] Rice, E. J., "Propagation of Waves in an Acoustically Lined Duct with a Mean Flow," *Basic Aerodynamic Noise Research*, NASA SP-207, 1969, pp. 345-355.

[22] Alfredson, R. J., "The Propagation of Sound in a Circular Duct of Continuously Varying Cross-Sectional Area," *Journal of Sound and Vibration*, Vol. 23, 1972, pp. 453-442.

[23] Beckemeyer, R. J., "Computational Methods for Analyzing Nonuniform Acoustic Waveguides," Ph.D. Dissertation, Univ. of Kansas, 1974.

[24] Beckemeyer, R. J. and Sawdy, D. T., "Analytical and Experimental Studies of Folded Cavity Duct Acoustic Liners," *92nd Meeting, Acoustical Society of America*, Paper YY11, San Diego, Calif., 1976.

[25] Sawdy, D. T. and Beckemeyer, R. J., "Transmission Loss of a Folded Cavity Liner as Predicted by an Extended Reaction Analysis," AIAA Paper 77-1358, Atlanta, Ga., 1977.